O.Ye. Loskutov,
I.S. Shponka,
O.O. Bondarenko,
N.S. Bondarenko,
A.G. Bozhko

HISTOLOGICAL AND HISTOCHEMICAL ASSESSMENT OF SHORT-TERM EVENTS IN PERIIMPLANT BONE FOR OSTEOINDUCTIVITY EVALUATION OF FUNCTIONAL-PROTECTIVE IMPLANT COATINGS

Dnipro State Medical University
V. Vernadsky str., 9, Dnipro, 49009, Ukraine
Дніпровський державний медичний університет
вул. В. Вернадського, 9, Дніпро, 49044, Україна
e-mail: olex.o.bondarenko@gmail.com

Abstract. Histological and histochemical assessment of short-term events in peri-implant bone for osteoinductivity evaluation of functional-protective implant coatings. Loskutov O.Ye., Shponka I.S., Bondarenko O.O., Bondarenko N.S., Bozhko A.G. *Utilization of functional-protective coatings for implants based on corundum ceramics seems promising from the point of view of stability, bioinertness, and low cost. In order to study the histological criteria for evaluating the osteoinductive properties of functional protective coatings, 6 types of coatings were studied on an experimental animal model: 90 Wistar rats were implanted with 6 test types of implants with various combinations of surface treatment (sand-blasting, surface treatment with a plasma torch with simultaneous application of aluminum oxide, powdered titanium, etc.) with an exposure of 1, 2 and 4 weeks. After euthanasia, a histological examination of decalcified bone with Masson-Goldner trichrome staining and TRAP-histochemical reaction for osteoclasts was performed. The obtained results demonstrated significantly higher osteoinductive properties of functional protective coatings with a more pronounced roughness ($R_a > 10$ µm) compared to an untreated titanium surface after 2 ($p < 0.01$) and 4 ($p < 0.05$) weeks of implantation. The corundum ceramic coating prevented the formation of implant wear particles, hence contributed to the stabilization of the newly formed bone. Therefore, the use of functional protective implant coatings based on corundum ceramics can increase the survival rate of conventional titanium implants, since the combination of factors such as surface roughness, mechanical stability, and chemical inertness of coatings with corundum ceramics provides better osteoinductive properties of implant materials.*

Реферат. Гістологічний і гістохімічних аналіз ранньострокових змін периімплантної кістки при оцінці остеоіндуктивних властивостей функціонально-захисних імплантних покриттів в експерименті. Лоскутов О.Є., Шпонька І.С., Бондаренко О.О., Бондаренко Н.С., Божко А.Г. *Використання функціонально-захисних покриттів імплантів на основі корундової кераміки виглядає перспективним з точки зору стійкості, біоінертності та невисокої вартості. З метою вивчення гістологічних критеріїв оцінки остеоіндуктивних властивостей функціонально-захисних покриттів було досліджено 6 типів покриттів на тваринній експериментальній моделі: 90 щурам лінії Wistar було імплантовано 6 досліджуваних типів імплантатів з різними комбінаціями обробки поверхні (струменевою обробкою поверхні карбідом кремнію, обробкою поверхні плазмовим пальником з одночасним нанесенням оксиду алюмінію, порошкового титану і т.д.) з експозицією 1, 2 і 4 тижні. Після евтаназії проводили гістологічне дослідження декальцинованої кістки із зафарбовуванням трихромом Массона-Голднера і гістохімічною реакцією на остеокласти. Отримані результати продемонстрували достовірно більш високі остеоіндуктивні властивості функціонально-захисних покриттів з більш вираженою шорсткістю ($R_a > 10$ мкм) порівняно з необробленою титановою поверхнею після 2 ($p < 0,01$) і 4 ($p < 0,05$) тижнів імплантації. Покриття з корундовою керамікою перешкоджало утворенню частинок зносу імпланта, що сприяло стабілізації новоствореної кістки. Таким чином, використання функціонально-захисних імплантних покриттів на основі корундової кераміки може підвищити виживаність конвенційних титанових імплантів, оскільки поєднання таких факторів, як шорсткість поверхні, механічна стійкість і хімічна інертність покриттів з корундовою керамікою забезпечує найкращі остеоіндуктивні якості матеріалів, що імплантуються.*

Bone tissue capacity to repair completely with full recovery of its histological architecture and function gave rise to miscellaneous successful approaches in bone injury treatment. Notwithstanding this advantage, the concept of a critical-size bone defect that cannot be healed without the use of assistive technologies has been introduced and actively developed in the last decades. Moreover, even with the smallest size of bone defect, the limiting factors of healing can be systemic and local adverse conditions, which require additional reparative approaches [15]. By this, the use of functional-protective coatings based on corundum ceramics for conventional titanium implants can be the key to successful peri-implant regeneration.

Reparative regeneration of any tissue requires the presence of three components, so-called "tissue triad": scaffold, cells and growth factors [13]. Their interaction can trigger, determine the sequence of events, and accomplish the programmed process of reparative regeneration. In this regard, the assessment of dynamics and quality of bone healing appears as a practical dilemma, which could be solved with adopting the fundamentals of osseous tissue repair biology that allow to find the weak points and appropriate methods of their correction. The current paradigm of peri-implant bone healing includes the basic processes of bone-implant interactions such as osteoinduction (implant-induced osteogenesis), osteoconduction (bone growth on an implant surface), and osseointegration

(direct anchorage of an implant) [1]. At the moment, there is a huge amount of publications about the morphological assessment of osseointegration, whereas the process of osteoinduction is underrepresented in reported histological studies. However, the importance of this phenomenon for evaluation of bone-implant interaction should not be underestimated, since osteoinduction precedes the osseointegration and determines its quality. Therefore, the objective of this study was to assess the histological hallmarks of the short-term events of peri-implant healing in experimental intramedullary bone defect, and to identify the impact of surface and compositional characteristics of functional and protective implant coatings on peri-implant regeneration, including the use of corundum ceramics.

MATERIALS AND METHODS OF RESEARCH

Implant materials. Cylindrical pins of 1.5 cm length and 1.5 mm in diameter were made from titanium wire (Grade 1 titanium alloy, Ukrainian: BT 1-00, Ti content ~ 99.6%). The surface of the wire was additionally treated by various methods: sandblasting with silicon carbide; surface treatment with a plasma torch with simultaneous coating with: A – titanium powder; B – corundum, type A25 (alumina content, Al_2O_3 ~ 99%), grain size 50 μm; C – sprayed titanium wire. All these treatment methods were combined with each other, in such a way that 6 different types of implant surfaces were modified for the experiment (Table).

Implant material characteristics, and their abbreviations

Implant material, coating	Abbreviation	Roughness (R_a, μm)
Untreated titanium wire	Ti	1.89
Ti + sandblasting	TS	4.87
TS + plasma with «A»	TSP	1.91
TS + plasma with «B»	TSPC	11.8
TS + plasma with «C»	TSPT	23.7
TS + plasma with «C» and «B»	TSPTC	11.5

After the corresponded treatment of titanium surface, the coated wire was cut into 15 mm cylindrical pins and sterilized at 135°C for 20 min immediately prior to experiment.

Animal model. The research was conducted in accordance with the Law of Ukraine "On Approval of the Procedure for Carrying Out Experiments on Animals "No. 249 of 03.01.2012 and requirements of "Directive 2010/63/EU of the European Parliament and of the Council of 22 September 2010 on the protection of animals used for scientific purposes as

amended by Regulation". The cylindrical pins were implanted intramedullary into the right femurs of 90 female Wistar rats with average age 17 weeks and weight 250 g. 15 more female Wistar rats were used as a sham operated control group. Animals were divided into 7 groups according to implant type (including sham operated group) and duration of implant exposure (1, 2 and 4 weeks). For anesthesia, a mixture of ketamine (80 mg/kg) and xylazine (8 mg/kg) was administered intramuscularly [11]. Skin was shaved and an incision of approximately 2 cm was made to the

right hind leg of the rats, on the lateral side of the knee. The knee joint was opened by making a 1-1.5 cm incision on the lateral side of the patella. The patella was then shifted medially, opening fossa inter-condylaris where a hole was drilled into the bone marrow cavity using a 1.5 mm drill. Then the bone marrow cavity was widened with a 1.6 mm trocar to 1.5 cm depth to insert an implant. During the operation, the knee joint was rinsed with phy-siological saline to keep the surface of the joint wet and to rinse out the debris such as bone dust from the drilling. The wound was closed with bio-degradable suture, treated with antiseptics and bandaged. Ketoprofen (15 mg/kg) was used for pain relief along with gentamicin (5 mg/kg) as an antibiotic during 5 days after surgery. All rats used the operated limb for locomotion after the surgery. Euthanasia was performed by intramuscular injec-tion of sodium thiopental, according to the established protocols [4].

Histological methods. After euthanasia, 1.5 cm fragments of the distal femurs with implants were collected. An electric saw (Dremel-2050, Germany) was used for this purpose, using a diamond-coated disk. The desired bone fragment was carefully sepa-rated from the implant and fixed in a 10% formalin buffered in PBS (pH=7.4) for at least 24 hours.

Decalcification was performed in 10% ethylene-diamine-tetraacetic acid (EDTA) solution, pH=7.4 at 4°C with agitation during 2 weeks [2]. Decalcified samples were embedded in paraffin and sectioned on rotary microtome HM340E (Thermo Scientific, Germany). 3-4 µm sections were stained using Mason-Goldner trichrome method [2]. Osteoclasts activity was revealed using histochemical detection of tartrate-resistant acid phosphatase (TRAP) by incubating sections for 30-60 min at 37°C in a substrate medium with 0.2% naphthol phosphate AS-BI (Sigma, Germany), 1% fast red-violet (Sigma, Germany) and 6% tartaric acid diluted in 0.2 M sodium acetate buffer solution (pH 4.8); fast green solution (Sigma, Ger-many) was used for the background staining [2]. Microscopy of all specimens was performed using an Axio Imager 2 microscope (Zeiss, Germany).

Statistics and morphometry. Morphometric ana-lysis was carried out with ZEN Software (Carl Zeiss AR, Germany). The thickness of peri-implant fibrous tissue was measured in 10 different fields of view (FOVs) under the magnification ×400 [2]. Measurement data were expressed as a median, first (25th percentile) and third (75th percentile) quartile (Q_1, Me, Q_3). Statistical analysis was performed using U-Mann-Whitney test (IBM SPSS Statistics 17.0, re-gistration number: 100-1D5AE), $p<0.05$ indicated significant and $p<0.01$ highly significant statistical

difference [10]. Box-and-whiskers plot diagram was drawn in online version of Microsoft Excel 2016.

RESULTS AND DISCUSSION

Sham operated group exhibited quite fast bone healing without installed implant material comparing to other investigated groups: fibrous tissue with sparse inflammatory cells predominantly replaced granulation tissue 1 week after intamedullar osteotomy; formation of cartilaginous tissue with osteogenesis on its peri-phery was demonstrated 2 weeks after the surgery; finally, within 4 weeks the experimental defect was completely replaced by newly formed bone trabeculae. Microscopical findings after 1 week of implant exposure were generally characterized by the presence of a scant inflammatory infiltrate and the ongoing organization of peri-implant hematoma. The inflam-matory infiltrate consisted mostly of macrophages blended with some lymphocytes and was located in the area of direct contact with the implant surface. Formation of granulation tissue was also observed in peri-implant site of all ivestigated specimens. The layer of peri-implant hematoma was defined as an accumulation of erythrocytes amidst homogeneous fibrin mass. Two different events were demostrated on the opposite boundaries of hematoma: inflammatory infiltrate was found closer to the implant; spindle-shaped and stellate fibroblasts appeared surrounded by the loose intercellular matrix from the side of preserved bone (Fig. 1). Comparative analysis of the described changes revealed no significant difference between investigated groups.

After 2 weeks of implantation period, histolo-gical findings were characterized by continuous decrease of inflammatory cells, the appearance of implant wear particles and the development of peri-implant fibrosis (Fig. 1). Noteworthy, the most conspicious amount of wear particles was observed in the groups with TS, TSPT and, to a lesser extent, in TSP. Multinucleated foreign-body cells were also found around the wear particles.

To compare the intensity of the fibroplastic reaction around the studied implants, the thickness of the peri-implant fibrous layer was evaluated. The narrowest fibrous layer (66 µm) was demonstrated in specimens with TSPTC, whereas the control group (Ti) revealed the most substantial fibrous layer formation (129 µm). In general, the groups with TSPC, TSPT and TSPTC showed significantly lower values of peri-implant fibrosis than in the control group with pure titanium ($p<0.01$). In other hand, TSPC, TSPT and TSPTC had no meaningful varia-tion between each other (Fig. 2). Similarly, there was no significant difference in the thickness of peri-implant fibrosis in the groups with TSP and TS comparing with the control group ($p>0.05$).
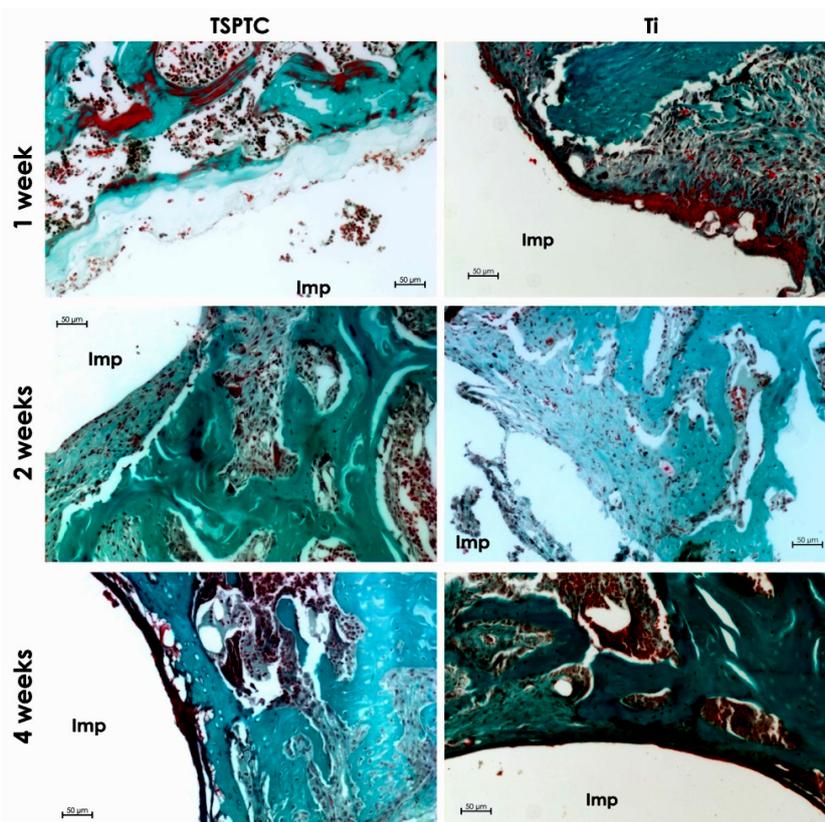
**Fig. 1. Dynamics of histological changes in the peri-implant area in the group
with corundum ceramics (TSPTC) and the control group (Ti). See text for explanation.
Imp – implant area. Masson-Goldner trichrome staining, ×200**

The general trend after 4 weeks of implantation period was characterized by decline of the fibrous layer thickness. The inflammatory infiltrate was absent, and the fibrous tissue itself was more compact with regular arrangement of collagen fibers and cells alongside the implant surfaces. Peri-implant osteogenesis was observed; furthermore, in some areas the bone trabeculae were aligned with the peri-implant fibrous tissue. The number of wear particles increased and they were observed in all study groups, though the lowest amount of them was found in TSPTC group. Comparative analysis of the intensity of the fibrous tissue development demonstrated thinner fibrous layers around the implants in TS, TSPC, TSPT and TSPTC groups compared with the control group; moreover, TSPT and TSPTC groups exhibited statistically significant difference with Ti group ($p<0.05$).
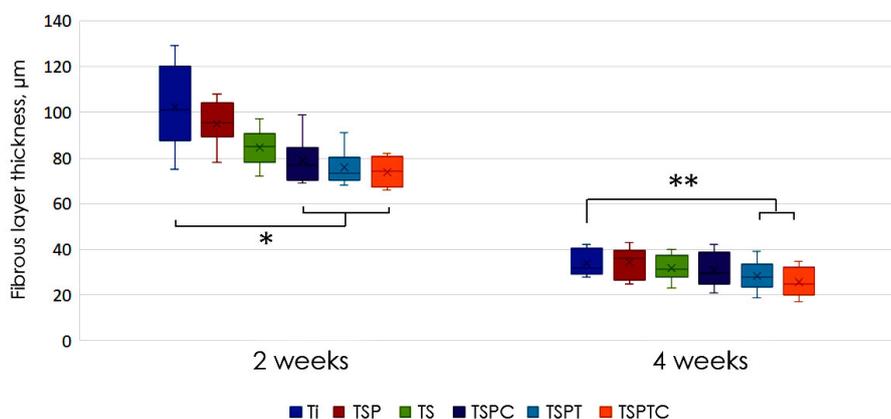

**Fig. 2. Comparison of peri-implant fibrosis among the investigated groups
after 2 and 4 weeks of implant exposure. * – $p<0.01$; ** – $p<0.05$**

Analysis of osteoclast activity displayed a general tendency to its increase in the peri-implant area after 4 weeks of implant exposure. However, no significant variation in osteoclast activity among the study groups was detected, although it is noticeable that the most active TRAP areas coincided with the presence of implant wear particles in nearby osseous tissue (Fig. 3).
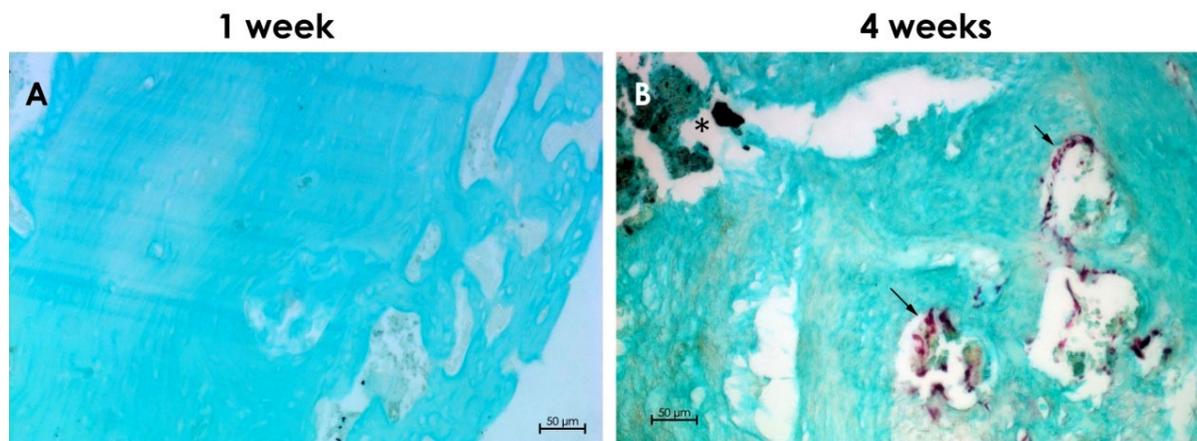

1 week   **4 weeks**

Fig. 3. Activity of osteoclasts in the peri-implant area of the TSPT group: no activity after 1 week (A), and (B) cluster of active osteoclasts (arrows) in the bone lacunae near the implantation site at 4 weeks of exposure (* - implant wear particles, metallosis). TRAP staining method, ×200

The obtained results demonstrated that histological changes in the peri-implant area completely correspond to the main stages of bone regeneration [5]. However, the chosen study timeframe for implant exposure did not approach the bone remodeling phase, which is generally could be confirmed by the low osteoclast activity. On the other hand, the first two phases are supposed to be accomplished in 3-4 days for the selected animal model, as was confirmed by histological findings in sham operated group.

Immediately after the formation of a bone defect, due to the damage of the bone vessels (and adjacent tissues), a hematoma is formed, which consists of peripheral and intramedullary blood cells, as well as bone marrow cells [8, 12]. Presumably, the primary implant instability makes this phase more prolonged in the investigated groups, since the limbs of the animals were not immobilized in the postoperative period. In the study groups, the inflammatory phase was also observed after 1 week. Polymorphonuclear leukocytes (PMN) belong to the cellular elements that play the greatest role in regeneration; they synthesize fibronectin and other structural proteins of the preliminary matrix, as demonstrated by Bastian et al. [9]. However, on histological slides that have been analyzed, the acute inflammatory response with a pronounced PMN infiltrate was predominantly absent after 7 days of implant exposure. In general, inflammatory infiltrate was represented by mononuclear leukocytes, mainly macrophages. Whereas macrophages are activated due to the injury in the acute phase, and consequently start to release the pro-inflammatory molecules; after a while, when a tissue debris is already resorbed, they become transformed into alternatively activated macrophages, synthesizing mainly growth factors necessary for regeneration [5].

The fibrovascular phase of healing is extremely important, because the fast revascularization provides the oxygen supply, delivery of nutrients, mediators and inflammatory cells [7]; whereas the formation of collagenous matrix initiates implant's stabilizing as well as it paves a road towards the osteogenesis. It is known that indirect healing of fractures consists of intramembranous and endochondral ossification, a key element of the latter is the formation of cartilage, which is later mineralized, resorbed and then replaced by newly formed bone. In the rat animal model, the peak of cartilage formation occurs 7-9 days after injury [3], which was also approved in our experiment in sham operated group, where a bone defect of 1.6 mm in diameter was healed via the cartilage formation between 7 and 14 day after the surgery. However, the cartilage formation in peri-implant area was not encountered in all investigated groups with the implants. Therefore, firstly, the actual size of experimental bone defect (1.5 cm length and 1.6 mm in diameter) can be considered as a highly adjacent to the critical-size bone defect; secondly, implant insertion reduces the bone defect, that lead to intramembranous osteogenesis due to the direct differentiation of osteoblasts from mesenchymal precursors, including, for instance, endosteal stem cells

which show exclusively osteogenic potential [14]. Consequently, a gradual thickness decrease of the peri-implant fibrous tissue between 2 and 4 weeks of implant exposure indicates its transformation into the newly formed bone tissue. Apparently, the average thickness of fibrous tissue around the implants is inversely dependent on the osteoinductive properties of the functional-protective coatings. Thus, implants coated with TSPC, TSPT and TSPTC possess significantly higher osteoinductive properties compared to conventional titanium implants with untreated surface. Nonetheless, in this study, the average roughness of the aforementioned implants (11.8, 23.7 and 11.5 μm, respectively) does not absolutely correlate with osteoinductive capability: implants with TSPT did not reveal the best osteoinductive properties, despite the highest surface roughness (R_a=23.7 μm). Hypothetically, the osteoconductive features of the implant could be determined by the chemical composition of the surface and its stability, and this hypothesis is indirectly confirmed by the detection of wear particles of implants (metallosis) in peri-implant sites, especially amidst TS, TSP and TSPT groups, i.e. groups with titanium coatings without corundum ceramics. Previous studies have shown that wear particles formed by friction between bone and implant reduce the transmission of antiosteoclastogenic signals through IL-6 and IFN-γ, activate osteoclasts through proinflammatory cytokines via the RANKL/RANK/OPG pathway, resulting in increasing level of osteoclasts and bone resorption; while the enhanced bone formation rather requires, on the contrary, for further osteointegration [6]. Displayed in our study elevated osteoclast activity near the deposits of such particles favors the theory mentioned above. Therefore, the use of functional-protective coatings with corundum ceramics can have advantages over the coatings composed of titanium powder and similar to them.

CONCLUSIONS

1. In a rat animal model with experimental femoral intramedullary osteotomy, a distal bone defect of 1.6 mm in diameter can be considered a critical-size bone defect, where the formation of cartilage could be still observed. The insertion of implant material with 1.5 mm in diameter modifies the type of bone healing from endochondral to intramembranous osteogenesis.

2. Osteoinduction, or the formation of bone tissue in response to implant insertion, starting at 2 weeks in an animal model in rats, can be assessed by the measurement of average thickness of fibrous tissue around the implant. The thickness of the peri-implant fibrous layer is inversely dependent on the implant's osteoinductive properties.

3. The investigated functional-protective coatings TSPC, TSPT and TSPTC secure the significantly higher osteoinductive properties (p<0.01) comparing with the untreated titanium surface after 2 weeks of implantation. Furthermore, the coatings of TSPT, TSPTC were significantly more osteoinductive than the untreated titanium surface after 4 weeks of implantation (p<0.05).

4. The use of functional-protective implant coatings based on corundum ceramics can increase the survival of conventional titanium implants, since the combination of factors such as surface roughness, mechanical stability and chemical inertness of corundum coatings provides the best osteoinductive features.

Conflict of interests. The authors declare no conflict of interest.

REFERENCES

1. Albrektsson T, Johansson C. Osteoinduction, osteoconduction and osseointegration. Eur Spine J. 2001 Oct;10 Suppl 2:S96-101. PMCID: PMC3611551. doi: https://doi.org/10.1007/s005860100282

2. An YH, Martin KL. Handbook of Histology Methods for Bone and Cartilage. Humana Press: Totowa; 2003.

3. Danoff JR, Aurégan JC, Coyle RM, Burky RE, Rosenwasser MP. Augmentation of Fracture Healing Using Soft Callus. J Orthop Trauma. 2016 Mar;30(3):113-8. doi: https://doi.org/10.1097/BOT.0000000000000481

4. AVMA Panel on Euthanasia. American Veterinary Medical Association. 2000 Report of the AVMA Panel on Euthanasia. J Am Vet Med Assoc. 2001 Mar 1;218(5):669-96. doi: https://doi.org/10.2460/javma.2001.218.669.

5. Bahney CS, Zondervan RL, Allison P, Theologis A, Ashley JW, Ahn J, Miclau T, Marcucio RS, Hankenson KD. Cellular biology of fracture healing. J Orthop Res. 2019 Jan;37(1):35-50. doi: https://doi.org/10.1002/jor.24170

6. Rony L, de Sainte Hermine P, Steiger V, Mallet R, Hubert L, Chappard D. Characterization of wear debris released from alumina-on-alumina hip prostheses: Analysis of retrieved femoral heads and peri-prosthetic tissues. Micron. 2018 Jan;104:89-94.
doi: https://doi.org/10.1016/j.micron.2017.11.002

7. Lu C, Marcucio R, Miclau T. Assessing angiogenesis during fracture healing. Iowa Orthop J. 2006;26:17-26. doi: https://pubmed.ncbi.nlm.nih.gov/20196645/

8. Marsell R, Einhorn TA. The biology of fracture healing. Injury. 2011 Jun;42(6):551-5. doi: https://doi.org/10.1016/j.injury.2011.03.031

9. Bastian OW, Koenderman L, Alblas J, Leenen LP, Blokhuis TJ. Neutrophils contribute to fracture healing by synthesizing fibronectin + extracellular matrix rapidly after injury. Clin Immunol. 2016 Mar;164:78-84. doi: https://doi.org/10.1016/j.clim.2016.02.001

10. Peacock J L, Peacock PJ. Oxford handbook of medical statistics. 2nd ed. Oxford University Press; 2020.

11. Rat and mouse anesthesia and analgesia. Formulary and general drug information. Animal Care and Use Program / University of British Columbia. Approved: march 2nd, 2016. Available from: https://animalcare.ubc.ca/sites/default/files/documents/GuidelineRodent20AnesthesianalgesiaFormulary28201629.pdf

12. Kolar P, Schmidt-Bleek K, Schell H, Gaber T, Toben D, Schmidmaier G, Perka C, Buttgereit F, Duda GN. The early fracture hematoma and its potential role in fracture healing. Tissue Eng Part B Rev. 2010 Aug;16(4):427-34. doi: https://doi.org/10.1089/ten.TEB.2009.0687

13. Payne KF, Balasundaram I, Deb S, Di Silvio L, Fan KF. Tissue engineering technology and its possible applications in oral and maxillofacial surgery. Br J Oral Maxillofac Surg. 2014;52(1):7-15. doi: http://dx.doi.org/10.1016/j.bjoms.2013.03.005

14. Vimalraj S, Arumugam B, Miranda PJ, Selvamurugan N. Runx2: Structure, function, and phosphorylation in osteoblast differentiation. Int J Biol Macromol. 2015;78:202-8. doi: https://doi.org/10.1016/j.ijbiomac.2015.04.008

15. Williams DL, Isaacson BM. The 5 hallmarks of biomaterials success: an emphasis on orthopaedics. Adv. Biosci. Biotechnol. 2014;5:283-293. doi: http://dx.doi.org/10.4236/abb.2014.54035

СПИСОК ЛІТЕРАТУРИ

1. Albrektsson T., Johanson C. Osteoinduction, osteoconduction and osseointegration. *Eur Spine J*. 2001. Vol. 10. P. S96-S101.
DOI: https://doi.org/10.1007/s005860100282

2. An Y. H., Martin K. L. Handbook of Histology Methods for Bone and Cartilage. Totowa: Humana Press, 2003.

3. Augmentation of Fracture Healing Using Soft Callus / J. R. Danoff et al. *J. Orthop. Trauma*. 2016. Vol. 30, No. 3. P. 113-118.
DOI: https://doi.org/10.1097/BOT.0000000000000481

4. AVMA Panel on Euthanasia. American Veterinary Medical Association. 2000 Report of the AVMA Panel on Euthanasia. *J. Am. Vet. Med. Assoc*. 2001. Vol. 218, No. 5. P. 669-696.
DOI: https://doi.org/10.2460/javma.2001.218.669

5. Cellular biology of fracture healing / C. S. Bahney et al. *J. Orthop. Res*. 2019. Vol. 37, No. 1. P.35-50.
DOI: https://doi.org/10.1002/jor.24170

6. Characterization of wear debris released from alumina-on-alumina hip prostheses: Analysis of retrieved femoral heads and peri-prosthetic tissues / L. Rony et al. *Micron*. 2018. Vol. 104. P. 89-94.
DOI: https://doi.org/10.1016/j.micron.2017.11.002

7. Lu C., Marcucio R., Miclau T. Assessing angiogenesis during fracture healing. *Iowa Orthop. J*. 2006. Vol. 26. P. 17-26.
URL: https://pubmed.ncbi.nlm.nih.gov/20196645/6

8. Marsell R., Einhorn T. A. The biology of fracture healing. *Injury*. 2011. Vol. 42, No. 6. P. 551-555.
DOI: https://doi.org/10.1016/j.injury.2011.03.031

9. Neutrophils contribute to fracture healing by synthesizing fibronectin + extracellular matrix rapidly after injury / O. W. Bastian et al. *Clin. Immunol*. 2016. Vol. 164. P. 78-84.
DOI: https://doi.org/10.1016/j.clim.2016.02.001

10. Peacock J. L., Peacock P. J. Oxford handbook of medical statistics. 2nd ed. Oxford University Press, 2020.

11. Rat and mouse anesthesia and analgesia. Formulary and general drug information. Animal Care and Use Program, 2nd ed / University of British Columbia. Approved: 2016. march,
URL: https://animalcare.ubc.ca/sites/default/files/documents/GuidelineRodent20AnesthesianalgesiaFormulary28201629.pdf

12. The early fracture hematoma and its potential role in fracture healing / P. Kolar et al. *Tissue Eng. Part B Rev*. 2010. Vol. 16, No. 4. P. 427-434.
DOI: https://doi.org/10.1089/ten.TEB.2009.0687

13. Tissue engineering technology and its possible applications in oral and maxillofacial surgery / K. F. Payne et al. *Br J Oral Maxillofac Surg*. 2014. Vol. 52. No. 1. P. 7-15.
DOI: http://dx.doi.org/10.1016/j.bjoms.2013.03.005

14. Vimalraj S., Arumugam B., Miranda P. J., Selvamurugan N. Runx2: Structure, function, and phosphorylation in osteoblast differentiation. *Int. J. Biol. Macromol*. 2015. Vol. 78. P. 202-208.
DOI: https://doi.org/10.1016/j.ijbiomac.2015.04.008

15. Williams D. L., Isaacson B. M. The 5 hallmarks of biomaterials success: an emphasis on orthopaedics. *Adv. Biosci. Biotechnol*. 2014. Vol. 5. P. 283-293.
DOI: http://dx.doi.org/10.4236/abb.2014.54035